Received: 1 February 2022 | Accepted: 8 May 2022

DOI: 10.1002/vzj2.20210

Vadose Zone Journal

ORIGINAL RESEARCH ARTICLE

Bias of stormwater infiltration measurement methods evaluated using numerical experiments

Nicholas P. Tecca[1] | **John Nieber**[2] | **John Gulliver**[1]

[1]Dep. of Civil, Environmental and Geo-Engineering, Univ. of Minnesota, Minneapolis, MN 55455, USA

[2]Dep. of Bioproducts and Biosystems Engineering, Univ. of Minnesota, St. Paul, MN 55108, USA

Correspondence
Nicholas P. Tecca, Dep. of Civil, Environmental and Geo-Engineering, Univ. of Minnesota, Minneapolis, MN 55455, USA.
Email: tecca001@umn.edu

Assigned to Associate Editor Thorsten Knappenberger.

Funding information
Minnesota Local Road Research Board; State of Minnesota, Department of Transportation, Grant/Award Number: Contract No. 1003325; Minneapolis-St. Paul Metropolitan Area (MSP) Urban Long Term Ecological Research Program; National Science Foundation, Grant/Award Number: DEB-2045382; USDA National Institute of Food and Agriculture, Hatch/Multistate, Grant/Award Number: Project MN 12–109

Abstract

Infiltration stormwater control measures (SCMs) have the potential to contribute towards mitigating the effects of urbanization on downstream receiving waters. Infiltration SCMs are most often successful when the in-situ saturated hydraulic conductivity (K_{sat}) is well characterized. In this paper numerical solutions of the Richards' equation are used to quantify the bias of seven infiltration measurement methods, removing natural variability and random error from the analysis. The methods evaluated in this study include the double ring infiltrometer, Saturo infiltrometer, modified Philip–Dunne infiltrometer, Turf-Tec IN2-W infiltrometer, USBR 7300-89 well permeameter, Philip–Dunne permeameter, and the Guelph permeameter. Seven homogenous, isotropic soil textures were simulated at four initial soil moistures for the seven methods, resulting in a total of 196 simulations. The dimensionless bias is defined as the "measured" K_{sat} determined by a given method divided by the K_{sat} input to the numerical experiments. The "measured" K_{sat} is in quotations to identify the measurement occurs in a numeric experiment rather than in a physical experiment. In sand through silt loam soils that are typical of infiltration SCMs, the simulated methods have a bias in the range of 0.7–6.2. The Turf-Tec was the only infiltrometer that produced a bias >2.5 for these soils. Initial effective saturation had a minimal contribution to bias for most methods. Methods that rely on a one-dimensional (1D) flow assumption consistently overestimated the K_{sat}. Borehole methods produced results with bias similar to surface methods. Long duration methods did not consistently produce more accurate results than short duration methods.

Abbreviations: DRI, double ring infiltrometer; GP, Guelph permeameter; H_{p0}, initial soil water pressure head; K_{sat}, saturated hydraulic conductivity; LSa, loamy sand; MPD, modified Philip–Dunne infiltrometer; PD, Philip–Dunne permeameter; Sa, sand; Saturo, Saturo infiltrometer by Meter Group; SaC, sandy clay; SaCL, sandy clay loam; SCM, stormwater control measure; Se, effective saturation; SiC, silty clay; SiL, silt loam; SaL, sandy loam; TT, Turf-Tec IN-2W infiltrometer; USBR, U.S. Bureau of Reclamation; WP, USBR 7300–89 well permeameter.

1 | INTRODUCTION

Infiltrating stormwater control measures (SCMs) have the potential to improve stormwater runoff water quality and reduce runoff volumes relative to urban systems without SCMs, particularly for small, frequent rain events. Infiltration SCMs include infiltration basins, infiltration trenches, infiltrating rain gardens, and bio-infiltration basins among other practices. Unfortunately, infiltration SCMs have a failure rate in the range of 10–50% (Bean & Dukes, 2016; CTC & Associates LLC, 2018; Hilding, 1994; Lindsey, et al., 1992). This failure rate represents a time period where the water quality and water quantity goals are not realized and as well as a significant capital expenditure to remediate the failure. One of the causes contributing to this failure is that the in-situ saturated hydraulic conductivity (K_{sat}) is often not well characterized. Some state jurisdictions allow soil texture to be used as a proxy for in-situ measures of K_{sat} (Minnesota Pollution Control Agency, 2018; Washington State Department of Ecology, 2014; Wisconsin Department of Natural Resources, 2017). However, the variability of K_{sat} within a soil texture group can exceed the variations between soil texture groups (Lee et al., 2016). Some state jurisdictions allow the in-situ infiltration measurement from a single point to be used for design (Minnesota Pollution Control Agency, 2018; North Carolina Department of Environmental Quality, 2020; Pennsylvania Department of Environmental Protection, 2006). However, soil properties can vary significantly across short distances even within a single soil order (Mulla & McBratney, 2001). Therefore, multiple measurements of K_{sat} are necessary to capture this natural heterogeneity even for relatively small infiltration SCMs (Asleson et al., 2009; Paus et al., 2014).

Regulating agencies often consider a variety of measurement methods to be acceptable (Minnesota Pollution Control Agency, 2017; Washington State Department of Ecology, 2014). However, there is limited information on the bias associated with each method.

Many factors can influence measured K_{sat} values in the field. Some factors can be controlled or corrected, such as influent temperature. Others present persistent problems that are not easily quantified, such as the influence of the chemical–physical condition of the sediment, soil structure, or entrapped air (Johnson, 1963). Emerson and Traver (2008) found that intra-annual variability of infiltration rate varied by roughly a factor of 2, resulting primarily from temperature-induced viscosity changes of the ponded water. Numerous studies have completed infiltration measurements using various methods, in various land uses, and found the range of measured values often exceeded an order of magnitude within a distance as short as 1 m (Asleson, et al., 2009; Gupta, et al., 2006; Munoz-Carpena, et al., 2002; Press, 2019; Reynolds, et al., 2000). The lack of an independent reference standard for which to compare field measured K_{sat} values is perhaps the greatest difficulty in assessing bias of infiltration measurement methods using field sites (Reynolds et al., 2000). It was therefore determined that the bias inherent to each infiltration measurement method could not be isolated from natural variability under field conditions.

Core Ideas

- Small infiltration tests with 3D flow corrections can be fast and accurate, requiring less water.
- Infiltration measurement methods that use a 1D flow assumption consistently overestimate K_{sat}.
- Infiltration tests achieve reasonable accuracy in <1.1 h in coarse soils typical of infiltration stormwater control measures.

There are two primary sources suspected to be contributing to bias in infiltration measurements. For methods that assume one-dimensional (1D) flow, the bias is likely due to the true flow path diverging laterally, creating an overestimation of the true K_{sat}. Alternatively, there are methods that account for the three-dimensional (3D) flow either through an assumed geometry or an empirical correction factor. The source of bias in these methods likely derives from a difference between the assumed and true flow geometries and may either underestimate or overestimate the true K_{sat}.

It is proposed to use a numerical solution of the Richards' equation to conduct numerical experiments of infiltration for each of the different infiltration methods and thereby remove the unknown natural variability of soils. Values of K_{sat} input to the numerical experiments would serve as an independent reference standard to assess bias. Such numeric simulations have been previously used to successfully evaluate individual infiltration measurement methods (Ahmed et al., 2014; Reynolds, 2010), unique soil conditions (Kindred & Reynolds, 2020), and SCM performance (Sasidharan et al., 2018). The limited scope of these previous studies does not allow for a simple comparison between methods. The objective of this study is to use numerical experiments to evaluate the bias of seven commonly used infiltration methods, removing spatial variability and other unknown sources of error associated with field measurements.

2 | METHODS

2.1 | Numerical solution procedure

The Subsurface Flow module within the COMSOL Multiphysics 5.4 software package was used to implement the

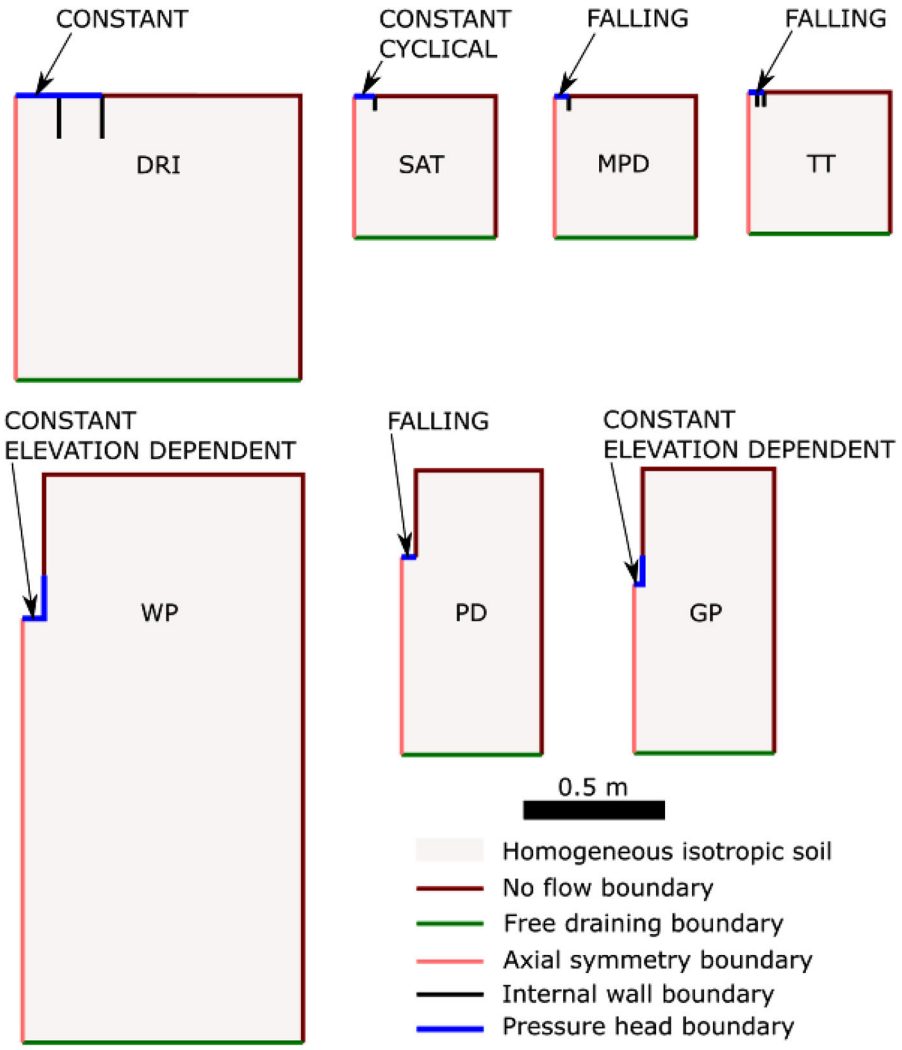

FIGURE 1 Geometry of the domain and boundary conditions for each simulated method. DRI, double ring infiltrometer; SAT, Saturo infiltrometer; MPD, modified Philip–Dunne infiltrometer; TT, Turf-Tech infiltrometer; WP, well permeameter USBR 7300–89; PD, Philip–Dunne permeameter; GP, Guelph permeameter

finite element solutions (COMSOL, 2020). All numerical experiments were conducted using time dependent numerical solutions. The variably saturated flow was assumed to be governed by the Richards' equation (Richards, 1931). A modified form of the van-Genuchten Mualem soil-water retention function was implemented following Vogel et al. (2001).

A two-dimensional axisymmetric domain was established for all numerical experiments. Half of each infiltrometer was placed in the domain, corresponding to the axisymmetry. The top boundary outside the infiltrometer and the outer vertical boundary were specified as a no flow condition, and the domain was sufficiently large such that the no flow boundaries did not influence the variably saturated flow from the simulated device. The bottom boundary, representing vertical flow to lower soil stratum, was defined as the unsaturated hydraulic conductivity under a unit hydraulic gradient, that is, was free draining. The constant head methods were prescribed using a constant pressure head boundary condition in the infiltration device. The falling head methods were specified by determining the cumulative time variable flux across the device boundary, converting it to an equivalent depth, and subtracting this equivalent depth from the initial head applied to the boundary. Rings that penetrated the soil domain were represented using an interior wall boundary condition. Boreholes were represented by removing the area of the borehole from the soil domain, with the appropriate boundary condition applied within the borehole. For uncased boreholes, the pressure head boundary condition was applied as a function of elevation within the borehole. A step function, smoothed to eliminate discontinuities in the first two derivatives, was used to smooth all sharp transitions in boundary conditions, including initialization and rapid changes in head, to facilitate solution convergence. See Figure 1 for the geometry of the domain and boundary conditions simulated for each

TABLE 1 Meshing parameters for each infiltration measurement method

Infiltration measurement method	No. of elements	Range of element sizes
		m
DRI	12,675	1×10^{-5}–0.025
Sat	1,271	1×10^{-3}–0.03
MPD	3,230	1×10^{-5}–0.025
TT	3,833	1×10^{-5}–0.025
WP	8,839	1×10^{-5}–0.05
PD	6,002	1×10^{-5}–0.025
GP	3,232	1×10^{-5}–0.05

Note. DRI, double ring infiltrometer; GP, Guelph permeameter; MPD, modified Philip-Dunne infiltrometer; PD, Philip–Dunne permeameter; SAT, Saturo infiltrometer; TT, Turf-Tech infiltrometer; WP, well permeameter USBR 7300–89.

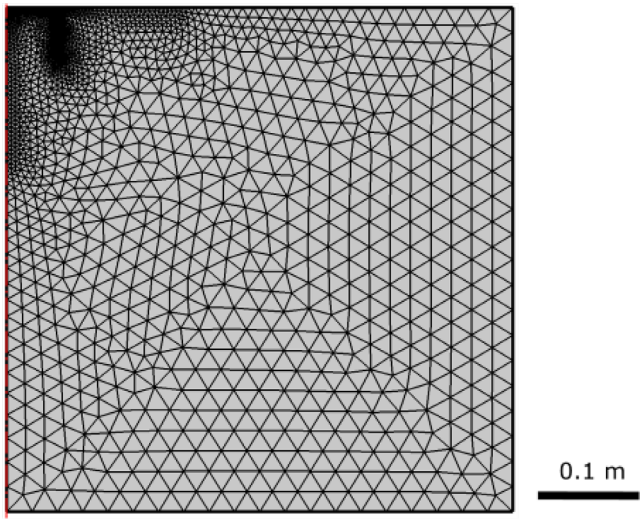

FIGURE 2 Modified Philip–Dunne infiltrometer mesh shown as an example of the mesh used for simulations

infiltration measurement method. Each infiltration measurement method was simulated using a finite element mesh as described by Table 1; an example mesh is shown for the modified Philip–Dunne infiltrometer (MPD) in Figure 2.

The soil physics moisture properties of seven different homogeneous, isotropic soils were specified as input to the simulations. While field soils are heterogeneous and anisotropic, the simplification to a homogeneous and isotropic soil domain provides an unambiguous reference standard to isolate the bias associated with each infiltration measurement method from other factors. The soil water retention characteristics (K_{sat}, α, n, θ_r, θ_s) of each specified soil texture was based on the mean value of each parameter following Carsel and Parrish (1988) and are displayed in Table 2. For all soil textures, the minimum capillary height (h_s) was set to −2 cm and the extrapolated water content parameter, θ_m, was calculated as a function of the soil water retention characteristics following (Vogel et al., 2001). Four different initial soil water pressure head (H_{p0}) conditions were defined for each soil texture. For coarse soils, the initial effective saturation (Se_0) varied from approximately 20–80% in 20% increments, with the usual definition of effective saturation being given by $Se = (\theta - \theta_r)/(\theta_s - \theta_r)$, where θ_r is the residual volumetric soil water content and θ_s is the saturated volumetric soil water content. Finer textured soils were limited to a maximum absolute value initial soil water pressure head of −10 m, in increments of 2.5 m. This was selected as clay soils in natural conditions would retain water and be relatively moist. In all cases, the initial effective saturation values covered a range of likely values on the soil-water retention function. Each combination of infiltration measurement method, soil texture, and initial soil moisture was implemented resulting in a total of 196 simulations (seven infiltration measurement methods, seven soil textures, and four initial soil moistures).

The bias is defined as the "measured" K_{sat} determined by the device procedure, divided by the K_{sat} input to the numerical experiment. The "measured" K_{sat} is in quotations to indicate the measurement occurred in a numeric experiment rather than in a physical soil. For the double ring infiltrometer and Turf-Tec infiltrometer, the quasi-steady-state infiltration rate is assumed to approach K_{sat} as the hydraulic gradient approaches unity. Therefore, a bias of 1 indicates the infiltration measurement method exactly calculated the input K_{sat} value. Bias of <1 indicates an underprediction of the input K_{sat}, while bias >1 indicates an overprediction.

2.2 | Infiltration measurement methods

A total of seven infiltration measurement methods were evaluated in this study. These methods were selected as they are either allowed by regulating agencies, well cited in the literature, or there is interest in adopting the method if it is shown to be reasonably accurate. The infiltration measurement methods evaluated in this paper are the double ring infiltrometer (DRI), Saturo by Meter Group (SAT), MPD, Turf-Tec IN2-W infiltrometer (TT), Well Permeameter USBR 7300-89 (WP), Philip–Dunne permeameter (PD), and Guelph permeameter (GP). These methods include both constant head and falling head methods. The observed variable for the constant head methods is the time variable flow rate, while the observed variable for the falling head methods is the time variable head. The output from the numerical experiments was post-processed following the procedure described by each method to determine a K_{sat} value. For methods that calculate infiltration rate rather than K_{sat}, the quasi-steady infiltration rate is typically assumed to be equal to K_{sat}. That assumption will be made herein.

The DRI as defined by ASTM International (2018b) is perhaps the most commonly implemented method for measuring

TABLE 2 Soil water retention function parameters associated with each simulated soil texture, based on the mean values from Carsel and Parrish (1988)

Soil texture	K_{sat}	α	n	θ_r	θ_s	H_{p0}	Se_0
	m s^{-1}	1 m^{-1}	–			m	
Sand	8.250×10^{-5}	14.5	2.68	0.045	0.43	−0.05	82%
						−0.0752	61%
						−0.1079	41%
						−0.1745	20%
Loamy sand	4.053×10^{-5}	12.4	2.28	0.057	0.41	−0.0589	82%
						−0.0958	61%
						−0.1499	41%
						−0.2762	20%
Sandy loam	1.228×10^{-5}	7.5	1.89	0.065	0.41	−0.1023	81%
						−0.1901	61%
						−0.3438	41%
						−0.7985	20%
Sandy clay loam	3.639×10^{-6}	5.9	1.48	0.1	0.39	−0.1682	81%
						−0.42	61%
						−1.0966	41%
						−4.7953	20%
Silt loam	1.250×10^{-6}	2	1.41	0.067	0.45	−0.5526	80%
						−1.5184	60%
						−4.5058	40%
						−10	29%
Sandy clay	3.333×10^{-7}	2.7	1.23	0.1	0.38	−0.7278	80%
						−3.2146	60%
						−7.5	50%
						−10	47%
Silty clay	5.556×10^{-8}	0.5	1.09	0.07	0.36	−2.5	93%
						−5	90%
						−7.5	87%
						−10	85%

Note. α, shape parameter; n, pore-size distribution parameter; θ_r, residual volumetric water content; θ_s, saturated volumetric water content; H_{p0}, initial soil water pressure head; Se_0, initial effective saturation.

infiltration rate. A constant head is maintained in two concentric rings, and the volumetric flow rate is measured in each ring. The volumetric flow rate of the inner ring is used to calculate the value of K_{sat} from the infiltration rate using a 1D flow assumption. The simulated test soil surface is contained within the 30-cm diam. inner ring, resulting in a horizontal test area of 706.9 cm^2.

The Saturo is a proprietary device that calculates the K_{sat} using a single ring infiltrometer and a dual head calculation procedure (Meter Group, 2019). The dual head procedure uses the measured steady-state infiltration rate at two different constant head levels. The Saturo documentation recommends two cycles of alternating high- and low-pressure head for wet soils, and three cycles for dry soils. Three cycles were used for all conditions herein. The recommended total run time varies from 75 to 180 min based on soil texture and moisture. The theory supporting the dual head procedure is based on the work of Reynolds and Elrick (1990) and Nimmo et al. (2009). The Saturo insertion ring has a 14.4-cm diam., resulting in a horizontal test area of 162.9 cm^2.

The MPD is an ASTM standard single ring falling head device that uses an optimization procedure to calculate the K_{sat} and Green-Ampt soil suction head (ASTM International, 2018a). The optimization uses the measured time variable head within the single ring, initial and final volumetric soil water content, Green-Ampt assumptions of a sharp wetting front, and an assumed capped spherical saturation zone geometry. The MPD simulations were completed with an initial ponding depth of 30 cm and were terminated when 30 cm of water had infiltrated or a maximum duration of 24 h. The

MPD uses a 10-cm diam. ring, resulting in a horizontal test area of 78.5 cm^2.

The TT is a small, falling head, double ring infiltrometer (Turf-Tec International, 2017). The TT has historically been used in the turf-management industry. However, the small size, ease of use, and minimal water requirement have generated interest in the TT. The TT uses a time-averaged 1D flow assumption to calculate the infiltration rate, which is assumed to approach K_{sat}, following an initial wetting period. In this paper, a 15-min wetting period and a 15-min testing period are used for all soil conditions as recommended by the Turf-Tec manual, although the user can vary this period based on the observed infiltration rate and user experience. The inner ring of the TT has a diameter of 6.03 cm, resulting in a horizontal test area of 28.6 cm^2.

The WP is a constant head borehole method completed in an uncased borehole (U.S. Bureau of Reclamation, 1989). The WP uses a steady-state flow assumption, and an empirical correction for the 3D flow including lateral flow through the uncased borehole. The WP can be completed with various configurations of well diameter and ponding depth. Following recommendations for a typical configuration, the WP was simulated with a 15-cm diam. borehole (177 cm^2 horizontal area) and a ponding depth of 15 cm.

The PD is a falling-head method implemented in a solid walled borehole (Philip, 1993). A spherical 3D flow geometry is assumed. The time variable head, initial and final volumetric soil moistures, an assumed spherical flow geometry, and borehole geometry are used to calculate the K_{sat} and soil suction head using an optimization procedure. The PD procedure applied within this paper uses the entire time variable head curve and a trust-region-reflective algorithm within a nonlinear least squares regression (MathWorks, 2022) to optimize the K_{sat} and soil suction head. The PD simulations were terminated when 30 cm of water have been infiltrated or a maximum duration of 24 h. The PD was simulated using a 10-cm diam. borehole (78.5 cm^2 horizontal area), although alternative diameters are possible.

The GP is a proprietary borehole device that calculates K_{sat}, soil sorptivity, and matrix flux potential in an uncased borehole (Soilmoisture Equipment Corp., 2012). The GP can calculate soil properties using either a single head or double head method, depending on the desired accuracy. This study implemented the more accurate double head method. The GP was originally described by Reynolds and Elrick (1986). Three-dimensional flow is accounted for by a shape factor that is a function of the soil microscopic capillarity length and therefore varies with soil texture as described by Zhang et al. (1998). The GP is simulated using a 6-cm diam. borehole (28.3 cm^2 horizontal area), and constant head depths of 10 and 20 cm.

Some important characteristics of each of the seven infiltration measurement methods are summarized in Table 3.

2.3 | Documented accuracy of infiltration methods

The seven infiltration methods discussed have varying levels of documentation on their respective accuracy. The DRI and MPD standards both indicate the measures are primarily for comparative use, that many factors influence the tests, and a quantitative statement on precision or bias is not provided (ASTM International, 2018a, 2018b). The Saturo is stated to have an accuracy of ±5% with respect to the measured infiltration rate (Meter Group, 2019), and therefore the K_{sat} that is calculated from the infiltration rate at two head levels will have a corresponding error. The GP states that the single head method can estimate K_{sat} within a factor of 2, and that the two head method is more accurate, but the accuracy of the two head method is not clearly documented (Soilmoisture Equipment Corp., 2012). The TT manual discusses accuracy and variation from lab measures as a result of the TT capturing field conditions such as vegetative cover and in-situ soil properties, but a quantitative statement regarding accuracy is not made (Turf-Tec International, 2017). Philip (1993) describes the PD procedure as approximate, although does not quantify the approximation. No statement on the accuracy of the WP could be located. The motivation of this work is to provide a quantitative estimate of the bias associated with each method and allow the relative accuracy to be compared between methods.

2.4 | Recommended K_{sat} range for each method

The recommended K_{sat} range of each infiltration measurement method was identified, when available. Table 4 describes which soils are likely to be well characterized by each infiltration measurement method based on the available documentation. Infiltration measurement methods are likely to be less accurate when implemented in a soil with hydraulic properties outside the recommended range.

2.5 | Determination of quasi-steady state

All numerical experiments completed in this study were for transient conditions, although four of the seven methods use a constant head flow condition and a steady-state assumption. A transient analysis is implemented to mimic the field measurement methods as closely as possible. Therefore, a criterion for quasi-steady state is required to determine when the method would be terminated if completed in the field. Of the four constant head methods, only the Saturo provides specific guidance on the duration of the test. The Saturo simulations were completed for three cycles alternating high-and low-pressure head, as recommended for dry soils, for each soil

TABLE 3 Comparison of selected infiltration measurement methods

Infiltration measurement method	Flow condition	Test arrangement	Assumed dimensionality	Measured property
DRI	Constant head	Surface	1D	Infiltration rate
SAT	Constant head	Surface	3D	K_{sat}
MPD	Falling head	Surface	3D	K_{sat}
TT	Falling head	Surface	1D	Infiltration rate
WP	Constant head	Borehole	3D	K_{sat}
PD	Falling head	Borehole	3D	K_{sat}
GP	Constant head	Borehole	3D	K_{sat}

Note. 1D, one-dimensional; 3D, three-dimensional; DRI, double ring infiltrometer; GP, Guelph permeameter; MPD, modified Philip-Dunne infiltrometer; PD, Philip–Dunne permeameter; SAT, Saturo infiltrometer; TT, Turf-Tech infiltrometer; WP, well permeameter USBR 7300–89.

TABLE 4 Recommended range of K_{sat} for the infiltration measurement methods and soil textures

Infiltration measurement method, recommended K_{sat} range	Sa	LSa	SaL	SaCL	SiL	SaC	SiC
	$K_{sat} = 8.25 \times 10^{-5}$ m s^{-1}	$K_{sat} = 4.053 \times 10^{-5}$ m s^{-1}	$K_{sat} = 1.228 \times 10^{-5}$ m s^{-1}	$K_{sat} = 3.639 \times 10^{-6}$ m s^{-1}	$K_{sat} = 1.25 \times 10^{-6}$ m s^{-1}	$K_{sat} = 3.333 \times 10^{-7}$ m s^{-1}	$K_{sat} = 5.556 \times 10^{-8}$ m s^{-1}
DRI, 1×10^{-7}–1×10^{-4} m s^{-1}	X	X	X	X	X	X	–
Saturo, 2×10^{-8}–3×10^{-4} m s^{-1}[a]	X	X	X	X	X	X	X
MPD, 6.9×10^{-7}–4×10^{-3} m s^{-1}	X	X	X	X	X	–	–
TT, 4.4×10^{-7}–3×10^{-4} m s^{-1}[b]	X	X	X	X	X	–	–
WP, 1×10^{-7}–1×10^{-3} m s^{-1}	X	X	X	X	X	X	–
PD, 6.9×10^{-7}–4×10^{-3} m s^{-1}[c]	X	X	X	X	X	–	–
GP, 1×10^{-7}–1×10^{-4} m s^{-1}	X	X	X	X	X	X	–

Note. DRI, double ring infiltrometer; GP, Guelph permeameter; MPD, modified Philip–Dunne infiltrometer; PD, Philip–Dunne permeameter; SAT, Saturo infiltrometer; TT, Turf-Tech infiltrometer; Sa, sand; LSa, loamy sand; SaL, sandy loam; SaCL, sandy clay loam; SiL, silty loam; SaC, sandy clay; SiC, silty clay; WP, well permeameter USBR 7300–89. An "X" and a "–" indicate the soil is within and outside the recommended K_{sat} range of the method, respectively.

[a]The range of K_{sat} is estimated from the range of infiltration rates, recommended difference in applied pressure head (Meter Group, 2019), and with a quasi-steady state Darcy's Law assumption.

[b]Clearly defined minimum and maximum values could not be located within Turf-Tec International (2017). The minimum and maximum values were estimated based on the device gradation, range of suggested monitoring durations, and the assumption that quasi-steady-state infiltration rate approaches K_{sat}.

[c]Clearly defined minimum and maximum values could not be located for the PD within Philip (1993). The minimum and maximum values were based upon values established for the MPD.

type and initial soil moisture. The GP does not provide a minimum required duration but recommends monitoring the rate of fall in the supply reservoir until the rate does not change significantly over three consecutive time intervals. The duration of the time intervals may vary from 2 to 15 min as the soils vary from coarse to fine. The GP does not clearly, quantitatively define what constitutes a significant change over a time interval. The DRI and WP have a 6-h minimum duration but recommend extending the test duration if the flow rate has not stabilized. In addition, the WP provides a minimum and maximum volume of water that should be infiltrated, but quantitative guidance on when to terminate the test between these volumes was not located. The guidance on the DRI and WP both refer to continuing the test until a relatively constant

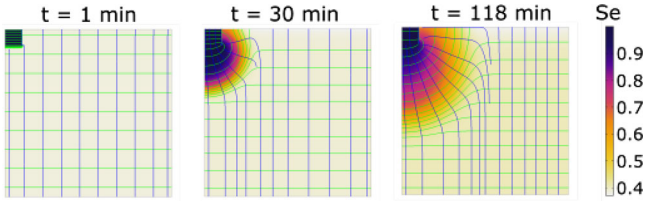

FIGURE 3 Example of the simulated change in effective saturation. The modified Philip–Dunne (MPD) method is simulated with a sandy loam soil and $Se_0 = 41\%$. The simulation terminated at 118 min when the simulated cylinder of water was completely drained. t, time; Se, effective saturation

flow rate is obtained, but do not provide quantitative guidance on what is sufficiently minimal change. The PD, MPD, and TT are falling head methods and therefore do not require an assumption of quasi-steady state.

This paper will implement a quasi-steady state criterion for the DRI, WP, and GP as a variation of flow of <1% over a duration of 15 min. The DRI and WP will use a minimum test duration of 6 h. The WP will also use the minimum water volume recommended in the method.

3 | RESULTS

The Richards' equation calculated the effective saturation throughout the model domain at each time step of the simulation. The effective saturation distribution influences the unsaturated hydraulic conductivity and the observed infiltration rate. Figure 3 shows the change in effective saturation for the MPD method over the simulation period as an example. All simulations were run on a single node with four cores and 8 GB of memory; the total run time for 196 simulations was 46 h, 5 min, 34 s.

Antecedent soil moisture is highly variable spatially and temporally in natural conditions. A dry antecedent soil moisture may require a longer test duration to achieve a steady-state condition. Figure 4 shows the bias as a function of the initial effective saturation for each of the seven infiltration measurement methods. It is observed that the variation in bias across initial effective saturation values within a soil texture class is relatively minimal for most soil textures except the silty clay. This indicates that the test durations are sufficient to allow a quasi-steady state to develop for the methods implementing a steady-state assumption, and that initial effective saturation is likely not a substantial source of bias. The TT is influenced the most by initial effective saturation, most notably in fine-textured soils. Tabulated results are given in supplemental material Supplemental Tables S1 through S7.

The duration of time required to take a measurement in the field is a metric approximating the difficulty of completing the measurement. Figure 5 shows the bias as a function of the duration of time that the test would be run in the field for each infiltration measurement method and soil texture. Tabulated results are given in supplemental material Supplemental Tables S1 through S7.

The bias of each simulation tends to get closer to 1 by extending the test duration, and the value plotted in Figure 5 is the time when the simulation was terminated. The trend of bias increasing with duration is a result of soils that are finer and drier requiring both a longer testing duration and having a higher bias than coarser or initially wetter soils. The duration of time in Figure 5 only includes the time when the method is actually infiltrating water, and excludes any time associated with assembly or disassembly in the field. Therefore, the results in Figure 5 should be considered comparative, between methods and soil textures, rather than an absolute statement on the duration required to complete each method.

As shown in Figures 4 and 5, the DRI performs consistently for all soil textures within the recommended K_{sat} range of the method. The DRI bias varies between 1.18 and 1.76 for soils sand through sandy clay that are within the recommended K_{sat} range. It is of note that all biases exceed 1 and are therefore nonconservative, in that the SCM will infiltrate below expectations. The DRI documentation (ASTM International, 2018b) does require a minimum test duration of 6 h and sandy clay and silty clay textured soils may require a duration in excess of 24 h to achieve steady state, as shown in Figure 5.

The Saturo performed well showing a bias in the range of 1.16–1.49 for sands through sandy clay soils. The maximum bias was 2.27 and occurred in a dry, silty clay. The Saturo was a relatively rapid test with durations varying between 115 and 180 min for all soil textures.

The MPD both underpredicted and overpredicted K_{sat}, with bias ranging from 0.95 to 1.08 when considering sand through silt loam soils that are within the recommended K_{sat} range of the method. The range of bias increased to 0.88–1.96 across all soil textures including those outside the recommended K_{sat} range and when less than the full water depth was infiltrated. The time required to infiltrate 30 cm of water, as shown in Figure 5, varied from 19 min for the sand to in excess of 24 h for the sandy clay and silty clay soil textures. The MPD would be a rapid test for sand and loamy sand soils with test durations <45 min. It would be less rapid for sandy loam and sandy clay loam soils, with test durations of approximately 2 and 6.5 h, respectively. Arrangements for longer duration tests would be required for silty loam, sandy clay, and silty clay soil textures.

The TT showed the greatest bias of any of the methods evaluated. The variability in the bias across initial soil moisture, within the same soil texture, was relatively minimal for coarse soils where infiltrating SCMs are likely to be constructed. The bias varied between 2.15 and 6.21 for soil textures from sand to silt loam. The maximum bias was 20.28 for the dry, silty clay. Two consecutive 15-min periods were implemented; therefore, all durations of the test are 30 min as shown in Figure 5.

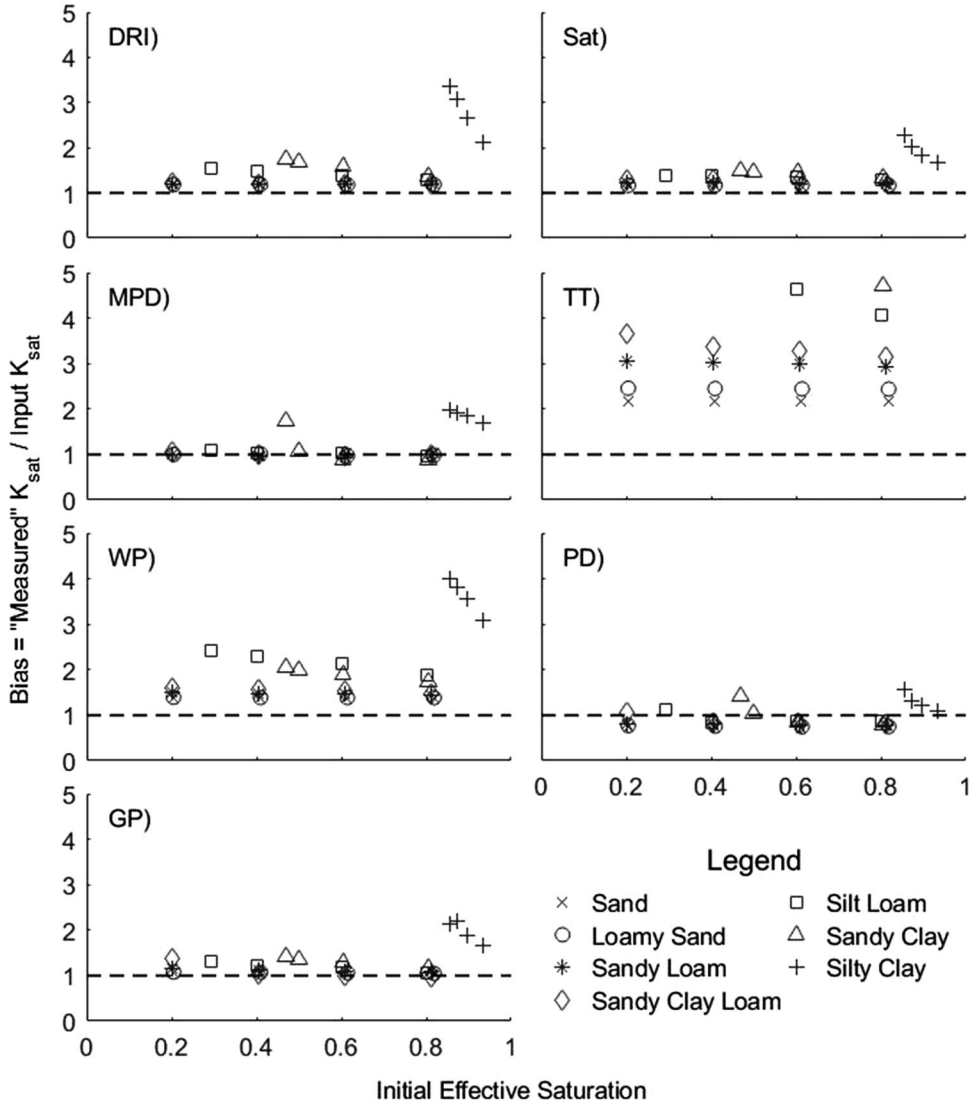

FIGURE 4 Bias as a function of initial soil moisture for each combination of method and soil type. There are silt loam, sandy clay, and silty clay points on the Turf-Tec (TT) subplot that exceed the displayed range of bias. DRI, double ring infiltrometer; SAT, Saturo infiltrometer; MPD, modified Philip–Dunne infiltrometer; TT, Turf-Tech infiltrometer; WP, well permeameter USBR 7300–89; PD, Philip–Dunne permeameter; GP, Guelph permeameter

The WP had bias ranging from 1.37 to 2.42 for sand through sandy clay soils that are within the recommended K_{sat} range of the method. The maximum bias was 3.98 for the dry, silty clay. The minimum duration of the test is 6 h. For the sandy clay and silty clay soil textures the method did not achieve either the quasi-steady state criteria or the minimum volume within the 24-h simulation.

The PD bias ranged from 0.73 to 1.14 for soil textures in the range from sand through silt loam that are within the recommended K_{sat} range. The full depth of water infiltrated within the maximum 24-h simulation duration for these soils. The range of bias increased from 0.15 to 1.58 across all soil textures including those outside the recommended K_{sat} range and when less than the full water depth was infiltrated.

The GP had a bias ranging from 0.95 to 1.41 for soils from sand through sandy clay that are within the recommended K_{sat} range. The bias increased to a maximum of 2.2 for the dry, silty clay, which is outside the recommended K_{sat} range. The test duration was relatively rapid ranging from 30 min in wet, sandy soils to a maximum of 9.85 h in dry, silty clay soils.

The DRI, WP, and GP all used a quasi-steady state criterion established by the authors to determine when to terminate the simulation. The standard method for the DRI and WP both require a 6-h minimum duration. The GP two head method does not have a minimum duration, but as the method is completed at two head levels and a 15-min window is required to establish quasi-steady state, 30 min is the shortest duration considered herein as illustrated in Figure 5. All three methods produce results at earlier times and appear to converge on

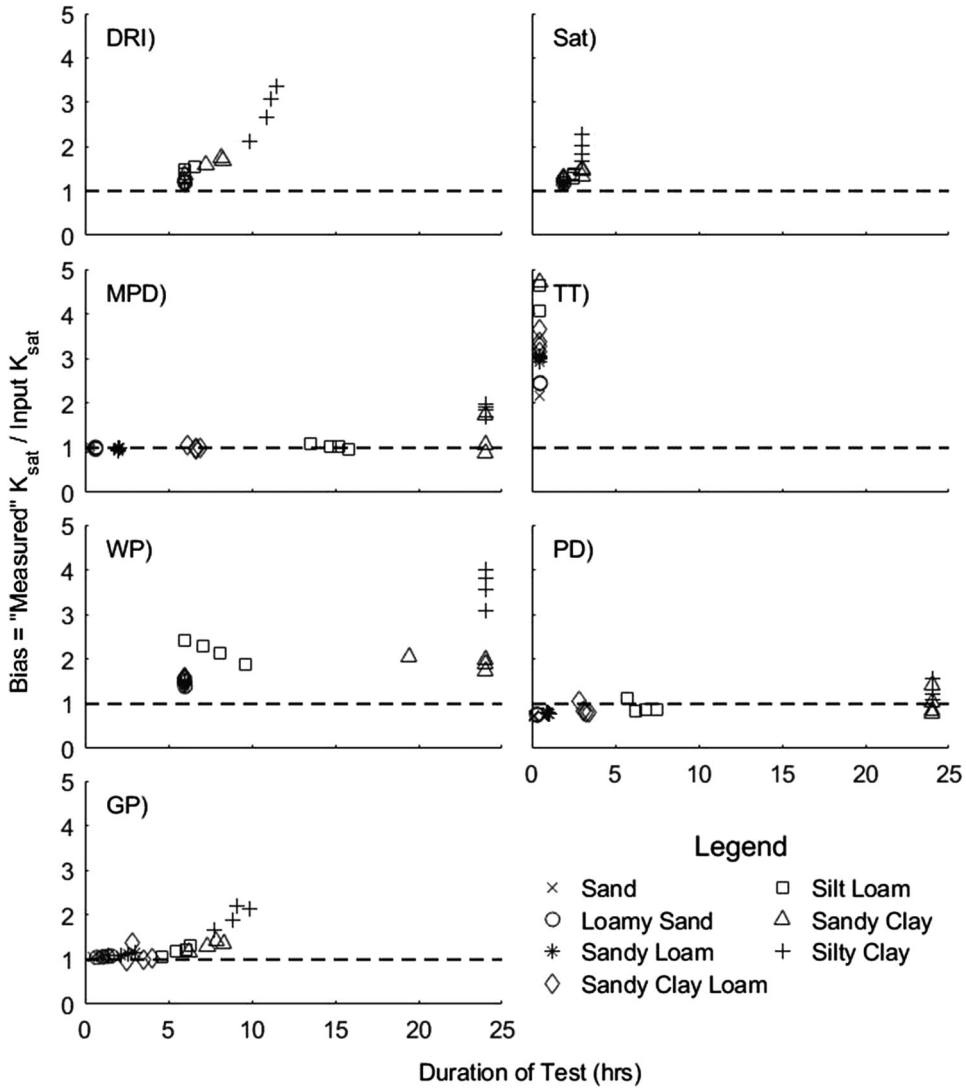

FIGURE 5 Bias as a function of test duration for each combination of method, soil type, and initial soil moisture. There are silt loam, sandy clay, and silty clay points on the Turf-Tec (TT) subplot that exceed the displayed range of bias. DRI, double ring infiltrometer; SAT, Saturo infiltrometer; MPD, modified Philip-Dunne infiltrometer; TT, Turf-Tech infiltrometer; WP, well permeameter USBR 7300–89; PD, Philip–Dunne permeameter; GP, Guelph permeameter

a steady state more rapidly than the 6-h minimum duration specified by the DRI and WP.

The DRI and WP specified minimum measurement time, or the WP specified minimum infiltrated volume may not be required for a given accuracy with a given soil. Figure 6 shows the bias of the DRI, WP, and GP over the first 6 h of the simulation. Coarse soils achieve a quasi-steady state much earlier in the test, converging rapidly with little variation between 1 and 6 h for each method. This may suggest that for coarse, high infiltration rate soils typical of infiltration SCMs, infiltration measurements can be terminated at a shorter duration. In the finer texture soils, the 6-h minimum seems appropriate and may need to be extended further to reach a quasi-steady-state condition. The variation of curvature in the GP time variable bias, displayed in Figure 6, corresponds to the differing shape factors associated with the coarse-textured soils, that is, sand, loamy sand, and sandy loam, and the finer-textured soils, that is, sandy clay loam, silt loam, sandy clay, and silty clay.

The Saturo method can produce an estimate of K_{sat} as soon as an infiltration rate is measured at each of the two head levels. As simulated, the Saturo method completed three cycles alternating between high head and low head, following the initial soak period. Figure 7 shows the variability of bias in response to the alternating head cycles over the simulation period for the Saturo. The general trend had the greatest bias at the beginning of a cycle, then it improved as the head was maintained and the infiltration rate stabilized. Later cycles tended to converge more rapidly than earlier cycles. The coarse soils showed minimal variability of bias, suggesting the Saturo provides relatively accurate results early in the

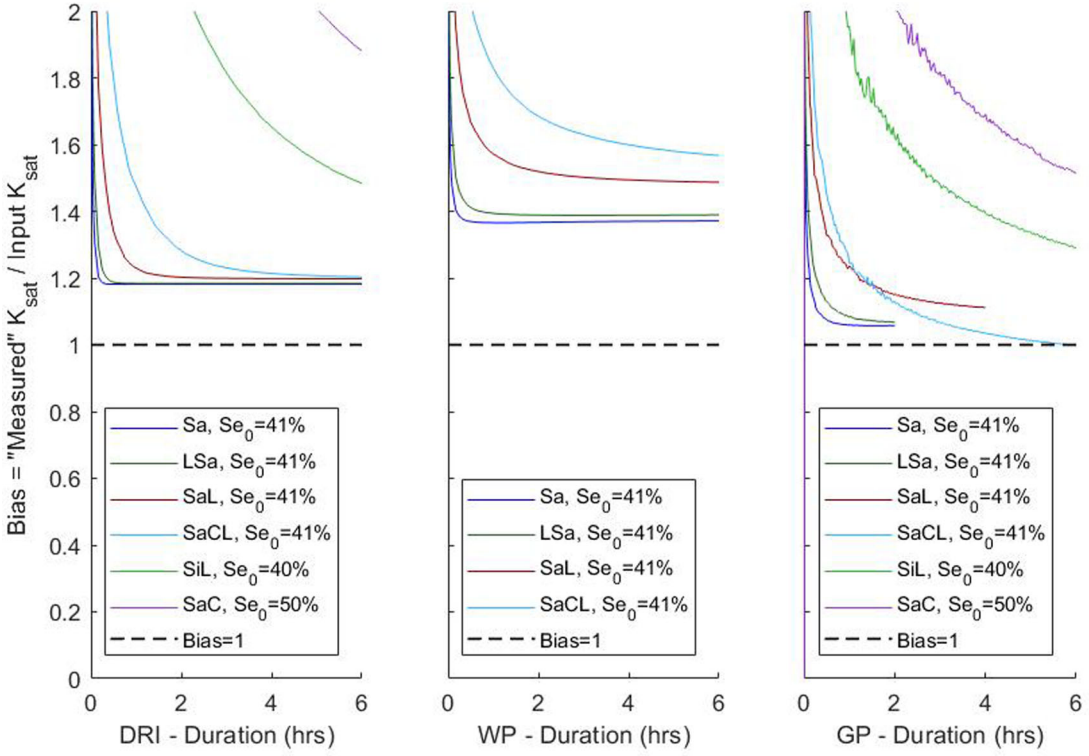

FIGURE 6 Variability of bias as a function of test duration for the double ring infiltrometer (DRI), well permeameter USBR 7300—89 (WP), and Guelph permeameter (GP). The silty clay (SiC) soil exceeds the displayed range of bias for the DRI and GP plots. Silt loam (SiL), sandy loam (SaC), and SiC soils exceed the displayed range of bias for the WP plot. Sa, sand; LSa, loamy sand; SaL, sandy loam; SaCL, sandy clay loam; Se_0, initial effective saturation

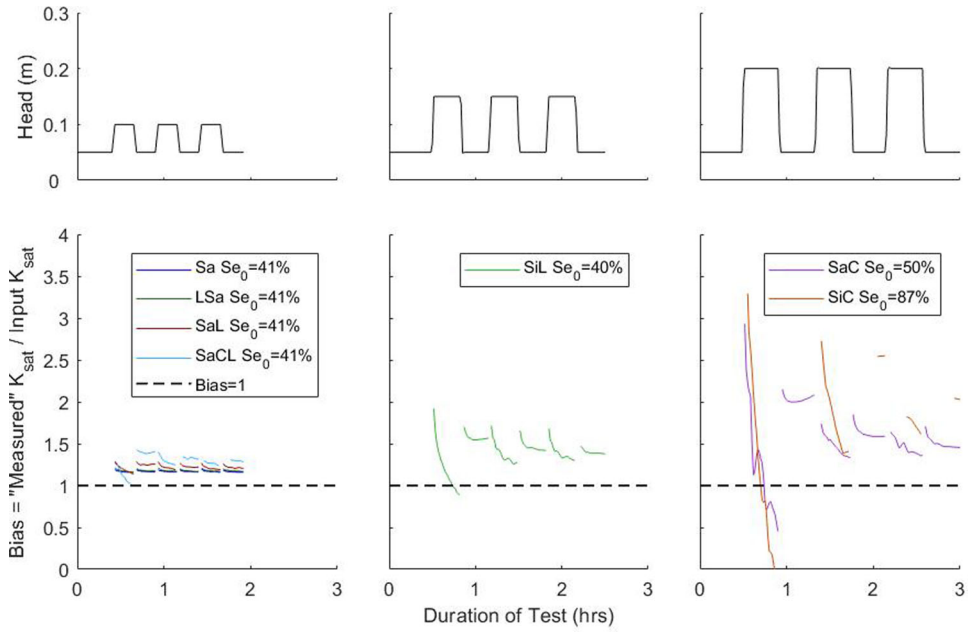

FIGURE 7 Variability of bias as a function of test duration for the Saturo. The saturated hydraulic conductivity (K_{sat}) is not calculated until an infiltration rate is available at both head levels. The Saturo cycles between two head levels as shown in the upper plots. The K_{sat} is not calculated during the transition between head levels. Discontinuities in the lines of a given soil texture occur at the change of head on the Saturo. Sa, sand; LSa, loamy sand; SaL, sandy loam; SaCL, sandy clay loam; SiL, silty loam; SaC, sandy clay; SiC, silty clay; Se_0, initial effective saturation

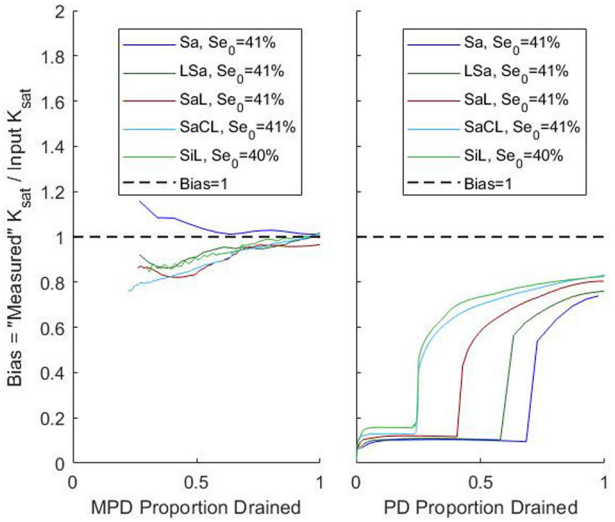

FIGURE 8 Variability of bias as a function of the proportion of the cylinder drained for the modified Philip–Dunne infiltrometer (MPD) and Philip–Dunne permeameter (PD). Sandy loam (SaC) and silty clay (SiC) soils did not drain completely within 24 h and are therefore not plotted. The MPD procedure requires the assumed capped spherical saturation zone to achieve a minimum radius and the optimization does not calculate a value prior to this minimum radius being achieved. Discontinuities in the slope of lines represent a shift in the optimization result. Sa, sand; LS, loamy sand; SaL, sandy loam; SaCL, sandy clay loam; SiL, silty loam; Se_0, initial effective saturation

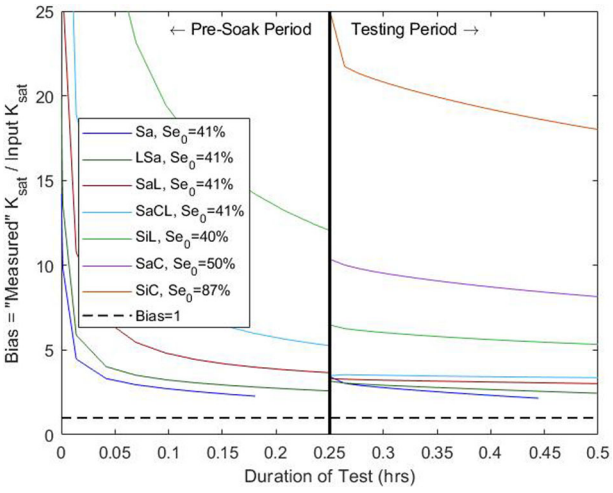

FIGURE 9 Variability of bias as a function of the test duration for the Turf-Tec infiltrometer (TT). The infiltration rate is not calculated during the step transition to refill the rings for the second 15-min interval, displayed as a vertical black line. The pre-soak period and testing period are to the left and right, respectively, of the vertical black line. The SaC and SiC curves exceed the plotted bias limits during the pre-soak period. Sa, sand; LSa, loamy sand; SaL, sandy loam; SaCL, sandy clay loam; SiL, silty loam; SaC, sandy clay; SiC, silty clay; Se_0, initial effective saturation

simulation period. Finer soils do appear to require the full recommended duration to achieve a reasonable result. The silt loam, sandy clay, and silty clay soils have a bias <1 during the first high head cycle, as shown in Figure 7. This is a result of the initial infiltration rate during the soak period being high, and the infiltration rate during the first high head cycle stabilizing to a lower infiltration rate than during the low head soak period. For the SaC and SiC soils the bias was calculated to be higher during the low head cycles than the high head cycles. This is likely caused by the time required for the soil water pressure to return to the low level.

As noted by Philip (1993), the PD, and by extension the MPD, are expected to produce the most accurate results when the cylinder is allowed to drain completely. However, the optimization procedure can be completed on a partial time series if a test is terminated prior to the cylinder draining completely. Figure 8 shows the bias as a function of the proportion of the cylinder allowed to infiltrate up to the cylinder draining completely. For both methods and across all soil textures, it appears the results are most accurate if more than 50–75%, depending upon soil texture, of the initial water volume in the cylinder is infiltrated, in this instance approximately 15–22.5 cm of the 30-cm initial depth. Philip (1993) notes that the assumed spherical geometry of the wetting front does not hold in the limit of small time, and therefore the reduced accuracy is to be expected when the volume infiltrated is less than the maximum for both the PD and MPD, as observed in Figure 8. The PD and MPD drained completely in as little as 9 and 19 min, respectively, for a dry sand representing a rapid method of estimating K_{sat}.

The TT simulation included a 15-min pre-soak period, followed by a 15-min testing period. In the case of the sand, the rings drained completely in <15 min. Figure 9 shows the variability in bias over the pre-soak period and the testing period. In the testing period, the bias is relatively stable after several minutes, except for the SC and SiC soil, implying the pre-soak and testing intervals are of sufficient duration for coarser soil. The bias may be reduced in the SC and SiC soils by extending the pre-soak period and testing period or adding additional testing periods.

4 | DISCUSSION

4.1 | One-dimensional flow assumption

The DRI and TT both rely on a 1D vertical flow assumption in the inner ring of the device. The goal of the outer ring is to buffer the divergent flow caused by the soil suction head in the adjacent unsaturated soil, allowing the inner ring flow to be purely vertical. Evaluating the flow net shows that while the flow in the outer ring is more divergent than the inner ring, the flow in the inner ring of both the DRI and TT is still laterally divergent. The effect is greater in the TT than the DRI, as the

TT has a smaller size and thus the lateral divergence accounts for a larger percentage of the infiltrated water.

Previous studies have indicated that larger diameter double ring configurations can provide reasonably accurate results. In a study on canal seepage where low infiltration rates would be anticipated, Robinson and Rohwer (1957) found that nested rings of 183 cm (6 ft) diam. and 549 cm (18 ft) diam. provided an accurate method of estimating infiltration rate. Lai and Ren (2007) found that a DRI with an inner ring of 80 cm and an outer ring of 100 cm reliably estimated K_{sat} in sandy loam, silt loam, and silt soil textures. The diameter of the inner ring, the ratio of the outer ring diameter to inner ring diameter, the ring penetration depth, and the soil texture all influence the assumption of 1D flow. A larger diameter inner ring is less susceptible to divergent flow, as the divergence would represent a proportionally smaller fraction of the total flow. A greater ratio of the outer ring diameter to the inner ring diameter would also decrease the bias, as the outer ring is increasingly able to buffer the background soil suction head. Finally, the rings provide a physical barrier to divergent flow while the water is within the soil column contained within the ring, thus a greater penetration depth forces 1D flow over a greater depth of soil. Finer and drier soils have a greater potential soil suction head, and therefore the bias would be expected to be larger as the texture transitions from coarse to fine and the initial soil moisture from wet to dry.

Johnson (1963) provides an early reference to the DRI configuration, including the 30- and 60-cm ring diam. and 15-cm penetration depth, now standardized in ASTM International (2018b). The author notes that divergent flow will influence measured infiltration rates, and states the proposed method is versatile and useful when considering economic limitations of larger tests. ASTM International (2018b) also likely considers the physical difficulty of installing larger rings. The preferred DRI installation method recommends using a jack under a truck, which is not practical for infiltration SCMs where driving on the soil surface is to be avoided.

4.2 | Three-dimensional flow corrections

The methods that implement a correction to account for the laterally divergent 3D flow rely on either an assumed geometry or a factor that corrects for the divergent flow paths. The PD uses an assumed spherical flow geometry, while the MPD uses an assumed capped spherical flow geometry. The SAT uses a factor that is a function of the insertion ring diameter and penetration depth. The WP uses a factor that is a function of ponded head, borehole radius, and the steady-state flow rate corrected to a standard water temperature. The GP uses a shape factor that is a function of the ponded head, borehole radius, and microscopic capillarity length following Zhang et al. (1998). The source of bias in these methods is likely due to the true flow path diverging from the simplifying assumptions of the method.

Philip (1993) discusses the idealized flow geometry as being more hydraulically efficient than the in-situ flow path. A factor of $8/\pi^2$ is introduced in the PD formulation, and subsequently the MPD, to account for this excess hydraulic efficiency. It is also of note that coarse soils are more likely to have flow that is dominated by gravity flow and have a larger vertical component, while finer soils likely have higher soil capillarity and therefore more lateral flow. This difference in flow geometry with soil texture likely introduces bias in methods that do not account for soil texture variation and may either underestimate or overestimate K_{sat}.

4.3 | Time required for measurement

The time required for a relatively accurate measurement of saturated hydraulic conductivity varies between infiltration devices. It also varies substantially between soil textures, and the finer soils require more time to reach a reasonable accuracy. To examine this, we will use sand as the reference soil texture and a bias within ± 0.2 of the final bias in a sand to represent the required time to achieve accuracy. The duration required to achieve a reasonable accuracy is shown in Table 5. Reasonable accuracy is achieved in <1.1 h for all infiltration measurement methods in the sand, loamy sand, and sandy loam textures. The duration increases in the finer texture soils. None of the infiltration measurement methods were able to achieve a reasonable accuracy within the simulated duration for the silty clay.

4.4 | Limitations of the current study

Numerical experiments are at best a representation of reality, but always deviate from the in-situ characteristics. The simulated domain was specified as isotropic and homogeneous to provide an unambiguous reference standard; however, this condition does not exist in nature. The simulations did not account for any soil structure, which can substantially influence the subsurface movement of water. The simulated domains also did not include any type of soil layering, which may result in different results in terms of bias.

The numerical experiments did not account for potentially imperfect implementation of the field procedures. Ring devices and borehole devices assume a tight seal is achieved with the soil interface, and a preferential flow path may exist if the seal is not sufficient. Borehole methods use an assumed geometry that may not be identical to the true borehole geometry and smearing of the soil may artificially decrease infiltration rates at the soil water interface. The application of water can suspend fines into the water column, which can clog open pore space, artificially reducing the measured infiltration potential. The sensitivity of specific types of sensors to

TABLE 5 Duration (h) required to achieve reasonable accuracy for each infiltration measurement method. Reasonable accuracy is defined as achieving a bias within ±0.2 of the final bias in a sand

Infiltration measurement method	Sa Se_0 = 41%	LSa Se_0 = 41%	SaL Se_0 = 41%	SaCL Se_0 = 41%	SiL Se_0 = 40%	SaC Se_0 = 50%	SiC Se_0 = 87%
DRI	0.1	0.2	0.5	1.3	9.4	17.7	>24
Saturo	0.4	0.4	0.4	0.4	1.3	1.7	>3
MPD	0.1	0.1	0.3	1.4	2.7	14.2	>24
TT	0.4	>0.5	>0.5	>0.5	>0.5	>0.5	>0.5
WP	0.1	0.2	1.1	5.7	>24	>24	>24
PD[a]	0.1	0.1	0.3	0.5	1.0	>24	>24
GP	0.1	0.2	0.8	1.0	7.0	>12	>24

Note. DRI, double ring infiltrometer; GP, Guelph permeameter; LSa, loamy sand; MPD, modified Philip-Dunne infiltrometer; PD, Philip–Dunne permeameter; Sa, sand; SAT, Saturo infiltrometer; SaC, sandy clay; SaCL, sandy clay loam; Se_0, initial effective saturation; SiC, silty clay; SiL, silty loam; SaL, sandy loam; TT, Turf-Tech infiltrometer; WP, well permeameter USBR 7300–89.

[a]Two exceptions to the PD results are sandy clay loam at Se_0 = 0.2 and silty loam at Se_0 = 0.29, where the bias of 1.06 and 1.14, respectively, is not within ±0.2 of the sand bias of 0.74.

detect small or large changes in water depth or flow rate was not evaluated. Long duration tests with ponded water may be influenced by evaporation, which was not included in the simulations. Finally, water temperature is important in evaluation the infiltration rate of soil (Emerson & Traver, 2008).

With these limitations in mind, the numerical experiments completed should be considered an idealized implementation of each method that allow for relative comparisons between methods. As the discussed limitations could result in either under- or overestimation, there is not likely a simple correction that can be applied to account for the various sources of natural variability and random error across all potential situations.

5 | CONCLUSIONS

There are many different methods to estimate soil hydraulic properties. When considering the soil where most infiltrating SCMs are located, that is sand through silt loam, the simulated methods had a bias in the range of 0.7–6.2. Methods that rely on a 1D flow assumption, including the DRI, consistently overestimate the infiltration rate. The TT was the only method where the bias exceeded 2.5 for soils from sand through silt loam. The range of bias appears to be reasonable given the natural heterogeneity of soil, but a correction should be considered, particularly for the TT, for engineering applications because otherwise a nonconservative error may be introduced.

All the infiltration measurement methods evaluated herein test a relatively small volume of soil. For many applications including infiltration SCMs, the soil properties need to be characterized over a much larger spatial extent than can be approximated by a single test. Multiple measurements are required to characterize the spatial heterogeneity of infiltration potential when the area of interest exceeds the extent of the tested soil volume (Ahmed et al., 2015). Methods that require less time and less water to estimate K_{sat} may be preferred to the conventional standard represented by the DRI.

When designing infiltration SCMs, it is important to understand the in-situ soil properties over the soil profile. Borehole methods of estimating hydraulic properties allow measurements to be completed at depth without expensive overexcavation. The three simulated borehole methods (i.e., WP, PD, and GP) produced results with similar levels of accuracy to the surface application methods and may be useful in characterizing vertical variations in K_{sat}.

The standard method for the DRI and WP rely on a steady-state assumption and have a minimum test duration of 6 h. As noted in Figure 6, the DRI and WP reach a quasi-steady state prior to the standard method minimum duration in many coarse materials. The Saturo, MPD, PD, GP all produce results of comparable accuracy to the DRI and WP, often with a shorter required duration. Selecting a test with a long duration or large water volume does not necessarily increase the accuracy of the measurement.

The TT produced the largest bias of the simulated methods. The range of bias was 2.15–6.21 for soil textures from sand to silt loam. However, the variability of K_{sat} between texture classes is often a factor of 5–10. This would suggest that the TT may be useful for differentiating between areas with high and low infiltration potential. The TT may be useful in applications where a rapid field test is required such as construction quality assurance applications, particularly when the surface being tested is known to be a coarse material. A correction factor in the range of 3–6 may be appropriate for soil materials in the range of sand to silt loam. For example, García-Serrana et al. (2018) found good simulation of swales after reducing the TT K_{sat} by a factor of 4.3, based upon field comparison measurements taken by J. Houle

(personal communication, 2017). The short duration and minimal water volume requirement of the TT test may allow for a large number of tests, corrected for bias, to be completed to characterize the variability of infiltration rate over an area.

The Saturo, MPD, PD, and GP were the most accurate methods for the silty clay soil texture. However, the MPD, PD, and GP require a substantially longer duration of test than the Saturo for fine soils, such as a silty clay, as shown in Figure 5. For coarser soils, the MPD, PD, and GP produce relatively accurate results with lower duration. The Saturo appears to be able to estimate the K_{sat} within a factor of 2.3 or less and with a duration of 3 h or less, which may be useful when exploring areas with limited knowledge of the soil characteristics.

Our suggestion is that the saturated hydraulic conductivity resulting from all infiltration measurement devices could be divided by the bias factor to account for the difference between the assumed flow geometry and the actual flow geometry. A bias factor of 1.2 is proposed for the 60 cm diam. double ring infiltrometer, 3 for the Turf-Tech infiltrometer, 1.4 for the well-head permeameter, 1.1 for the Guelph permeameter, 1.2 for the Saturo, 0.8 for the PD, and 1.0 for the MPD. The Saturo, PD, GP, and the MPD were relatively accurate for sandy clay and more course soil textures. The double ring infiltrometer was relatively accurate for the silt loam and coarser soils. The well permeameter was relatively accurate for the sandy clay loam and coarser soils. There was no evaluated infiltration measurement device that could accurately quantify the saturated hydraulic conductivity of silty clay within the simulated duration.

ACKNOWLEDGMENTS

The authors acknowledge the Minnesota Supercomputing Institute (MSI) at the University of Minnesota for providing resources that contributed to the research results reported within this paper. URL: http://www.msi.umn.edu. This paper is based on the results of a project supported by the Minnesota Local Road Research Board under the authority of the State of Minnesota, Department of Transportation Contract No. 1003325. This work was also made possible, in part, by the Minneapolis-St. Paul Metropolitan Area (MSP) Urban Long Term Ecological Research Program, through its grant from the National Science Foundation (DEB-2045382). John L. Nieber's effort on this project was partially supported by the USDA National Institute of Food and Agriculture, Hatch/Multistate Project MN 12–109.

AUTHOR CONTRIBUTIONS

Nicholas P. Tecca: Conceptualization; Formal analysis; Investigation; Methodology; Visualization; Writing – original draft. John Nieber: Conceptualization; Funding acquisition; Methodology; Software; Supervision; Writing – original draft; Writing – review & editing. John Gulliver: Conceptualization; Funding acquisition; Project administration; Supervision; Writing – original draft; Writing – review & editing.

CONFLICT OF INTEREST

The authors declare no conflict of interest.

ORCID

Nicholas P. Tecca https://orcid.org/0000-0002-0438-5513
John Nieber https://orcid.org/0000-0001-9630-3935

REFERENCES

Ahmed, F., Gulliver, J. S., & Nieber, J. L. (2015). Field infiltration measurements in grassed roadside drainage ditches: Spatial and temporal variability. *Journal of Hydrology*, *530*, 604–611. https://doi.org/10.1016/j.jhydrol.2015.10.012

Ahmed, F., Nestingen, R., Nieber, J. L., Gulliver, J. S., & Hozalski, R. M. (2014). A modified Philip–Dunne infiltrometer for measuring the field-saturated hydraulic conductivity of surface soil. *Vadose Zone Journal*, https://doi.org/10.2136/vzj2014.01.0012

Asleson, B. C., Nestingen, R. S., Gulliver, J. S., Hozalski, R. M., & Nieber, J. L. (2009). Performance assessment of rain gardens. *Journal of the American Water Resources Association*, *45*(4), 1019–1031. https://doi.org/10.1111/j.1752-1688.2009.00344.x

ASTM International. (2018a). Standard practice for measuring field infiltration rate and calculating field hydraulic conductivity using the modified Philip Dunne infiltrometer test. *ASTM International*, D8152-18. https://doi.org/10.1520/D8152-18

ASTM International. (2018b). Standard test method for infiltration rate of soils in field using double-ring infiltrometer. *ASTM International*, D3385-18. https://doi.org/10.1520/D3385-18

Bean, E. Z., & Dukes, M. D. (2016). Evaluation of infiltration basin performance on coarse soils. *Journal of Hydrologic Engineering*, *21*(1), 1–9. https://doi.org/10.1061/(ASCE)HE.1943-5584.0001258

Carsel, R. F., & Parrish, R. S. (1988). Developing joint probability distributions of soil water retention characteristics. *Water Resources Research*, *24*(5), 755–769. https://doi.org/10.1029/WR024i005p00755

COMSOL. (2020). *Multiphysics v. 5.4* COMSOL AB. https://www.comsol.com/support/knowledgebase/1223

CTC & Associates LLC. (2018). *Infiltration basins: Standards and procedures to ensure performance*. Minnesota Department of Transportation. http://dot.state.mn.us/research/TRS/2018/TRS1801.pdf

Emerson, C. H., & Traver, R. G. (2008). Multiyear and seasonal variation of infiltration from storm-water best management practices. *Journal of Irrigation and Drainage Engineering*, *134*(5), 598–605. https://doi.org/10.1061/(ASCE)0733-9437(2008)134:5(598)

García-Serrana, M., Gulliver, J. S., & Nieber, J. L. (2018). Calculator to estimate annual infiltration performance of roadside swales. *Journal of Hydrologic Engineering*, *23*(6), 04018017. https://doi.org/10.1061/(asce)he.1943-5584.0001650

Gupta, N., Rudra, R. P., & Parking, G. (2006). Analysis of spatial variability of hydraulic conductivity at field scale. *Canadian Biosystems Engineering*, *48*(1), 55–62.

Hilding, K. (1994). Longevity of infiltration basins assessed in Puget Sound. *Watershed Protection Techniques*, *1*(3), 124–125.

Johnson, A. I. (1963). A field method for measurement of infiltration. *Geological Survey Water-Supply Paper*, *1544-F*, 27.

Kindred, J. S., & Reynolds, W. D. (2020). Using the borehole permeameter to estimate saturated hydraulic conductivity for glacially over-consolidated soils. *Hydrogeology Journal*, *28*(5), 1909–1924. https://doi.org/10.1007/s10040-020-02149-3

Lai, J., & Ren, L. (2007). Assessing the size dependency of measured hydraulic conductivity using double-ring infiltrometers and numerical simulation. *Soil Science Society of America Journal*, *71*(6), 1667–1675. https://doi.org/10.2136/sssaj2006.0227

Lee, R. S., Traver, R. G., & Welker, A. L. (2016). Evaluation of soil class proxies for hydrologic performance of in situ bioinfiltration systems. *Journal of Sustainable Water Built Environment*, *2*(4), 1–10. https://doi.org/10.1061/JSWBAY.0000813

Lindsey, G., Roberts, L., & Page, W. (1992). Inspection and maintenance of infiltration facilities. *Journal of Soil and Water Conservation*, *47*(6), 481–486.

MathWorks. (2022). *lsqnonlin solve nonlinear least-squares (nonlinear data-fitting) problems*. Mathworks. https://www.mathworks.com/help/optim/ug/lsqnonlin.html

Meter Group. (2019). *Saturo*. Meter Group. http://library.metergroup.com/Manuals/20496_SATURO_Manual.pdf

Minnesota Pollution Control Agency. (2017). *Minnesota stormwater manual*. Minnesota Pollution Control Agency. https://stormwater.pca.state.mn.us/index.php/Main_Page

Minnesota Pollution Control Agency. (2018). *Construction stormwater general permit*. Minnesota Pollution Control Agency. https://www.pca.state.mn.us/sites/default/files/wq-strm2-80a.pdf

Mulla, D. J., & McBratney, A. B. (2001). Soil spatial variability. In Warrick, A. W. (Ed.), *Soil physics companions* (pp. 343–373). CRC Press.

Munoz-Carpena, R., Regalado, C. M., Alvares-Benedi, J., & Bartoli, F. (2002). Field evaluation of the new Philip-Dunne permeameter for measuring saturated hydraulic conductivity. *Soil Science*, *167*(1), 9–24. https://doi.org/10.1097/00010694-200201000-00002

Nimmo, J. R., Schmidt, K. M., Perkins, K. S., & Stock, J. D. (2009). Rapid measurement of field-saturated hydraulic conductivity for areal characterization. *Vadose Zone Journal*, *8*, 142–149. https://doi.org/10.2136/vzj2007.0159

North Carolina Department of Environmental Quality. (2020). *Stormwater design manual*. North Carolina Department of Environmental Quality. https://deq.nc.gov/about/divisions/energy-mineral-and-land-resources/stormwater/stormwater-program/stormwater-design

Paus, K. H., Morgan, J., Gulliver, J. S., Leiknes, T., & Hozalski, R. M. (2014). Assessment of the hydraulic and toxic metal removal capacities of bioretention cells after 2 to 8 years of service. *Water, Air, and Soil Pollution*, *225*(1), 1–12. https://doi.org/10.1007/s11270-013-1803-y

Pennsylvania Department of Environmental Protection. (2006). *Pennsylvania stormwater best management practices manual*. Pennsylvania Department of Environmental Protection. http://www.depgreenport.state.pa.us/elibrary/GetFolder?FolderID=4673

Philip, J. R. (1993). Approximate analysis of falling-head lined borehole permeameter. *Water Resources Research*, *29*(11), 3763–3768. https://doi.org/10.1029/93WR01688

Press, J. (2019). *Determining the minimum number of single-ring infiltration tests required to reliably predict performance of a rain garden* [Master's thesis, Villanova University].

Reynolds, W. D. (2010). Measuring soil hydraulic properties using a cased borehole permeameter: Steady flow analyses. *Vadose Zone Journal*, *9*, 637–652. https://doi.org/10.2136/vzj2009.0136

Reynolds, W. D., Bowman, B. T., Brunke, R. R., Drury, C. F., & Tan, C. S. (2000). Comparison of tension infiltrometer, pressure infiltrometer, and soil core estimates of saturated hydraulic conductivity. *Soil Science Society of America Journal*, *64*(2), 478–484. https://doi.org/10.2136/sssaj2000.642478x

Reynolds, W. D., & Elrick, D. E. (1986). A Method for simultaneous in situ measurement in the vadose zone of field-saturated hydraulic conductivity, sorptivity and the conductivity-pressure head relationship. *Groundwater Monitoring & Remediation*, *6*(1), 84–95.

Reynolds, W. D., & Elrick, D. E. (1990). Ponded infiltration from a single ring: I. Analysis of steady flow. *Soil Science Society of America Journal*, *54*, 1233–1241. https://doi.org/10.2136/sssaj1990.03615995005400050006x

Richards, L. A. (1931). Capillary conduction of liquids through porous mediums. *Physics*, *1*(5), 318–333. https://doi.org/10.1063/1.1745010

Robinson, A. R., & Rohwer, C. (1957). Measurement of canal seepage. *Transactions of the American Society of Civil Engineers*, *122*(1), 347–363. https://doi.org/10.1061/taceat.0007491

Sasidharan, S., Bradford, S. A., Šimůnek, J., DeJong, B., & Kraemer, S. R. (2018). Evaluating drywells for stormwater management and enhanced aquifer recharge. *Advances in Water Resources*, *116*(November 2017), 167–177. https://doi.org/10.1016/j.advwatres.2018.04.003

Soilmoisture Equipment Corp. (2012). *Guelph permeameter – Operating instructions*. Soilmoisture Equipment Corp.

Turf-Tec International. (2017). *Turf-Tec infiltrometer IN-2 instructions*. Turf-Tec International.

U.S. Bureau of Reclamation. (1989). *Procedure for performing field permeability testing by the well permeameter method 7300–89*. U.S. Bureau of Reclamation.

Vogel, T., van Genuchten, M. T., & Cislerova, M. (2001). Effect of the shape of the soil hydraulic functions near saturation on variably-saturated flow predictions. *Advances in Water Resources*, *24*, 133–144. https://doi.org/10.1016/S0309-1708(00)00037-3

Washington State Department of Ecology. (2014). *Stormwater management manual for western Washington*. Washington State Department of Ecology. https://fortress.wa.gov/ecy/madcap/wq/2014SWMMWWinteractive/2014.SWMMWW.htm

Wisconsin Department of Natural Resources. (2017). *Conservation practice standard 1002 site evaluation for stormwater infiltration*. Wisconsin Department of Natural Resources. https://dnr.wi.gov/topic/stormwater/documents/1002SiteEvalForInfiltr.pdf

Zhang, Z. F., Groenevelt, P. H., & Parkin, G. W. (1998). The well-shape factor for the measurement of soil hydraulic properties using the Guelph permeameter. *Soil and Tillage Research*, *49*(3), 219–221. https://doi.org/10.1016/S0167-1987(98)00174-3

SUPPORTING INFORMATION

Additional supporting information can be found online in the Supporting Information section at the end of this article.

How to cite this article: Tecca, N. P., Nieber, J., & Gulliver, J. (2022). Bias of stormwater infiltration measurement methods evaluated using numerical experiments. *Vadose Zone Journal*, *21,* e20210. https://doi.org/10.1002/vzj2.20210